THE JOURNAL OF BIOLOGICAL CHEMISTRY
Vol. 276, No. 24, Issue of June 15, pp. 21698–21703, 2001
Printed in U.S.A.

Partial Reconstitution of Photoreceptor cGMP Phosphodiesterase Characteristics in cGMP Phosphodiesterase-5*

Received for publication, January 23, 2001, and in revised form, March 15, 2001
Published, JBC Papers in Press, April 2, 2001, DOI 10.1074/jbc.M100626200

Alexey E. Granovsky‡ and Nikolai O. Artemyev§

From the Department of Physiology and Biophysics, University of Iowa College of Medicine, Iowa City, Iowa 52242

Photoreceptor cGMP phosphodiesterases (PDE6) are uniquely qualified to serve as effector enzymes in the vertebrate visual transduction cascade. In the dark-adapted photoreceptors, the activity of PDE6 is blocked via tight association with the inhibitory γ-subunits (Pγ). The Pγ block is removed in the light-activated PDE6 by the visual G protein, transducin. Transducin-activated PDE6 exhibits an exceptionally high catalytic rate of cGMP hydrolysis ensuring high signal amplification. To identify the structural determinants for the inhibitory interaction with Pγ and the remarkable cGMP hydrolytic ability, we sought to reproduce the PDE6 characteristics by mutagenesis of PDE5, a related cyclic GMP-specific, cGMP-binding PDE. PDE5 is insensitive to Pγ and has a more than 100-fold lower k_{cat} for cGMP hydrolysis. Our mutational analysis of chimeric PDE5/PDE6α′ enzymes revealed that the inhibitory interaction of cone PDE6 catalytic subunits (PDE6α′) with Pγ is mediated primarily by three hydrophobic residues at the entry to the catalytic pocket, Met^{758}, Phe^{777}, and Phe^{781}. The maximal catalytic rate of PDE5 was enhanced by at least 10-fold with substitutions of PDE6α′-specific glycine residues for the corresponding PDE5 alanine residues, Ala^{608} and Ala^{612}. The Gly residues are adjacent to the highly conserved metal binding motif His-Asn-*X*-*X*-His, which is essential for cGMP hydrolysis. Our results suggest that the unique Gly residues allow the PDE6 metal binding site to adopt a more favorable conformation for cGMP hydrolysis.

cGMP phosphodiesterases (PDE6)[1] play the role of effector enzymes in the vertebrate visual transduction cascade. In retinal rod cells, photoexcited rhodopsin induces GDP/GTP exchange on the visual G protein, transducin (Gt), and liberated Gtα·GTP activates PDE6. A homologous cascade operates in cone photoreceptors. cGMP hydrolysis by active PDE6 results in the closure of cGMP-gated channels in the plasma membrane (1, 2). The key attributes of the visual cascade, low noise and high gain signal amplification, place specific requirements on PDE6. The enzyme must have a very low basal cGMP hydrolytic rate in the dark-adapted photoreceptors and a very high catalytic rate in the transducin-activated state. This is achieved through two unique features of PDE6: the inhibitory interaction of the catalytic subunits with the γ-subunit and an exceptionally high k_{cat} value for cGMP hydrolysis when the inhibition is turned off.

The lack of a practical expression system for PDE6 (3–5) has stalled the progress in determining the structural basis of PDE6 function. We have begun to study the structure and function relationship of PDE6 by constructing chimeras between cone PDE6α′ and cGMP binding cGMP-specific PDE (PDE5 family) (5, 6). PDE5 and PDE6 display a high degree of identity (45–48%) between the catalytic domains, a strong substrate selectivity for cGMP, and similar sensitivity to a common set of competitive inhibitors (7–9). Yet, the reported maximal rate of cGMP hydrolysis by PDE5 catalytic dimers is only ~10 moles of cGMP per mole of PDE·sec, which is ~400–550-fold lower than the k_{cat} estimates for PDE6 (5, 10–15). Furthermore, the activity of PDE5 is unaffected by the PDE6 γ-subunit (5, 6). This, and a robust functional expression of PDE5 using the baculovirus/insect cell system (16), makes PDE5 a valuable tool for "gain of PDE6 function" experiments. Recently, we have shown that a substitution of the segment PDE5-(773–820) by the corresponding PDE6α′-(737–784) sequence in the wild-type PDE5 or in a PDE5/PDE6α′ chimera containing the catalytic domain of PDE5 results in chimeric enzymes capable of inhibitory interaction with Pγ (6). Alanine-scanning mutational analysis of the previously identified Pγ cross-linking site, PDE6α′-(750–760) (17), revealed a critical Pγ-interacting residue, Met^{758} (6). In a model of the PDE6α′ catalytic domain, Met^{758} faces the opening of the catalytic cavity (6). We then hypothesized that Pγ may interact with additional nonconserved residues located at the perimeter of the cavity, thus allowing Pγ to serve as a lid on the catalytic pocket. In this study, we mutated three candidate Pγ contact residues identified from the model of PDE6α′ and examined these mutants for inhibition by Pγ.

The rationale for our search of the catalytic determinants of PDE6 was based on biochemical evidence and the crystal structure of the PDE4 catalytic domain (18–20), which suggests the critical role of the two highly conserved metal binding motifs, His-Asn-*X*-*X*-His (I) and His-Asp-*X*-*X*-His (II), in the hydrolysis of cyclic nucleotides. We replaced PDE6α′ domains containing motifs I and II into PDE5. Resulting chimeric PDEs and corresponding mutants have been analyzed to test our hypothesis.

EXPERIMENTAL PROCEDURES

Materials—cGMP was obtained from Roche Molecular Biochemicals. [^{3}H]cGMP was a product of Amersham Pharmacia Biotech. All restriction enzymes were purchased from New England Biolabs. AmpliTaq® DNA polymerase was a product of PerkinElmer Life Sciences, and Pfu DNA polymerase was a product of Stratagene. Rabbit polyclonal His-

* This work was supported by National Institutes of Health (NIH) Grant EY-10843. The services provided by the Diabetes and Endocrinology Research Center of the University of Iowa were supported by NIH Grant DK-25295. The costs of publication of this article were defrayed in part by the payment of page charges. This article must therefore be hereby marked "*advertisement*" in accordance with 18 U.S.C. Section 1734 solely to indicate this fact.

‡ Recipient of the American Heart Association Heartland Affiliate Predoctoral Fellowship.

§ Established Investigator of the American Heart Association. To whom correspondence should be addressed. Tel.: 319-335-7864; Fax: 319-335-7330; E-mail: nikolai-artemyev@uiowa.edu.

[1] The abbreviations used are: PDE, cGMP phosphodiesterase; Pγ, γ-subunit of PDE6; PDE6α′, α′-subunit of cone PDE6; PDE5, cGMP binding, cGMP-specific PDE (PDE5 family); PCR, polymerase chain reaction; HPLC, high performance liquid chromatography.

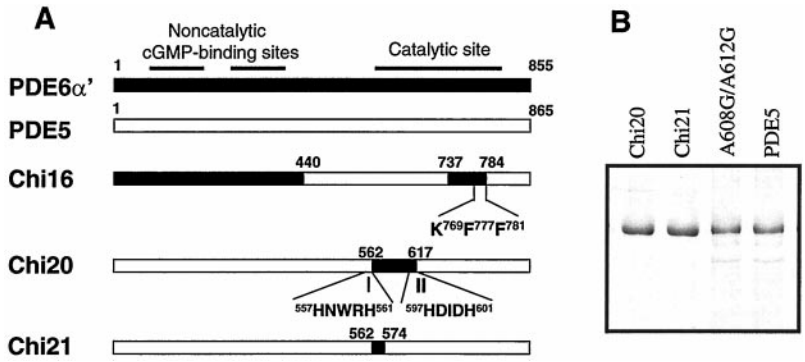

FIG. 1. **Construction and expression of PDE5/PDE6α′ chimeras and mutants in Sf9 cells.** *A,* schematic representation of PDE5/PDE6α′ chimeras. The PDE6α′ residues substituted by Ala in Chi16 and the metal binding motifs I and II are shown. The PDE6 and PDE5 motifs I are identical. *B,* an SDS-polyacrylamide gel (12%) of purified PDE5, Chi20, Chi21, and PDE5A608G/A612G (2 μg per lane) stained with Coomassie Blue. The recombinant His_6-tagged proteins were expressed in Sf9 cells and partially purified using chromatography on a His-Bind resin and HPLC on a Mono Q® HR 5/5 column as described under "Experimental Procedures."

probe (H-15) antibodies were purchased from Santa Cruz Biotechnology. Zaprinast and all other reagents were purchased from Sigma.

Cloning of Pγ Mutants—Pγ mutants were generated based on the pET11a-Pγ expression vector (21, 22). Residues Ile^{86} and Ile^{87} were substituted for alanine using PCR-directed mutagenesis. PCR products were obtained using a forward primer containing a *Nde*I site and a reverse primer containing the mutations and a *Bam*HI site. The fragments were digested with *Nde*I/*Bam*HI and subcloned into the pET11a-Pγ digested with the same enzymes.

Preparation of Pγ and Pγ Mutants—The Pγ-subunit and its mutants were expressed in *Escherichia coli* and purified on a SP-Sepharose fast flow column and on a C_4 HPLC column (Microsorb-MW, Rainin) as described (22). Purified proteins were lyophilized, dissolved in 20 mM HEPES buffer, pH 7.5 and stored at −80 °C until use.

Cloning of Chi20 and Chi21—The constructs for expression of PDE5/PDE6α′ chimeras were obtained based on pFastBacHTb-PDE5 vector (5). To obtain Chi20 and Chi21, original restriction sites in pFastBacHTb-PDE5, *Spe*I and *Sph*I, were eliminated and re-introduced at desired positions to allow a site-directed cloning of PDE6α′ fragments into PDE5. To eliminate two *Spe*I restriction sites located within the 3′-untranslated region of PDE5 cDNA and the unique *Sph*I site from the multiple cloning sequence of the vector, pFastBacHTb-PDE5 was digested with *Spe*I/*Sph*I and treated with mung bean nuclease. New *Spe*I and *Sph*I restriction sites (PDE5 codons for Arg^{606}-His^{607}-Ala^{608} and Ala^{618}-Leu^{619}-Lys^{620}, respectively) were introduced into the vector using a QuikChange™ kit (Stratagene). To obtain Chi21 (Fig. 1), a synthetic olygonucleotide duplex, encoding for PDE6α′-(561–574), was ligated into the modified pFastBacHTb-PDE5 vector digested with *Spe*I and *Sph*I. To generate Chi20, a PCR fragment, encoding for PDE6α′-(575–617), was digested with *Spe*I/*Blp*I and subcloned into the modified pFastBacHTb-PDE5 vector digested with *Spe*I/*Blp*I(partial). The resulting construct was digested with *Spe*I/*Sph*I and ligated to the synthetic oligonucleotide duplex encoding for PDE6α′-(561–574).

Site-directed Mutagenesis of PDE5 and Chi16—Site-directed mutagenesis of PDE5 was performed using a QuikChange™ kit. A pair of complementary oligonucleotides encoding for the Ala^{608}→Gly and Ala^{612}→Gly substitutions (PDE5A608G/A612G) was used to PCR-amplify the pFastBacHTb-PDE5 vector. The PCR product was treated with *Dpn*I to eliminate the template and was transformed into *E. coli* DH5α. Chi16 mutants with single substitutions of residues Lys^{769}, Phe^{777}, and Phe^{781} by Ala were constructed using PCR-directed mutagenesis. A unique *Nhe*I site (PDE5 codons for Pro^{661}-Leu^{662}) was introduced into Chi16 using a QuikChange™ kit. The 5′-primer sequence included the *Nhe*I recognition site. Reverse primers contained a desired mutation and the *Stu*I site. The PCR products were digested with *Nhe*I/*Stu*I and subcloned into the modified Chi16 vector cut with the same enzymes. Sequences of all mutants were verified by automated DNA sequencing at the University of Iowa DNA Core Facility.

Expression and Purification of Recombinant PDEs and their Mutants—Sf9 cells were harvested at 60 h after infection, washed with 20 mM Tris-HCl buffer, pH 7.8 containing 50 mM NaCl, and resuspended in the same buffer containing a protease inhibitor mixture (10 μg/ml pepstatin, 5 μg/ml leupeptin, and 0.2 mM phenylmethylsulfonyl fluoride). The cell suspensions were sonicated using 30-s pulses for a total duration of 3 min. The supernatants (100,000 × *g*, 45 min) were loaded onto a column with a His-Bind resin (Novagen) equilibrated with 20 mM Tris-HCl buffer, pH 7.8, containing 10 mM imidazole. The resin was washed with a 5× volume of the buffer containing 500 mM NaCl and 25 mM imidazole. Proteins were eluted with the buffer containing 250 mM imidazole. β-mercaptoethanol (2 mM) was added to the eluate. PDE5, Chi20, Chi21, and PDE5A608G/A612G were additionally purified using ion-exchange chromatography on a Mono Q® HR 5/5 column (Amersham Pharmacia Biotech). Purified proteins were dialyzed against 40% glycerol and stored at −20 °C.

Other Methods—PDE activity was measured using [^{3}H]cGMP as described (23, 24). Less than 15% of cGMP was hydrolyzed during these reactions. The K_i values for inhibition of PDE activity by Pγ and zaprinast were measured using 0.5 μM cGMP (*i.e.* <35% of the K_m value for chimeric and mutant PDEs). Protein concentrations were determined by the method of Bradford (25) using IgG as a standard or by using calculated extinction coefficients at 280 nm. The molar concentrations of Chi20, Chi21, and mutatnt PDEs, [PDE], were calculated based on the fraction of PDE protein in preparations, and the molecular mass of 93.0 kDa. The fractional concentrations of PDE were determined from analysis of the Coomassie Blue-stained SDS gels using a HP ScanJet II CX/T scanner and Scion Image Beta 4.02 software. A typical fraction of Chi16 mutants in partially purified preparations was 10–15%. A typical fraction of purified Chi20, Chi21, and PDE5A608G/A612G was 65–70%. The k_{cat} values for cGMP hydrolysis were calculated as V_{max}/[PDE]. SDS-polyacrylamide gel electrophoresis was performed by the method of Laemmli (26) in 10–12% acrylamide gels. For Western immunoblotting, proteins were transferred to nitrocellulose (0.1 μm, Schleicher & Schuell) and analyzed using rabbit His-probe (H-15) or sheep anti-PDE6α′ antibodies (5, 6, 27). The antibody-antigen complexes were detected using anti-rabbit or anti-goat/sheep IgG conjugated to horseradish peroxidase and ECL reagent (Amersham Pharmacia Biotech.). Fitting the experimental data to equations was performed with nonlinear least squares criteria using GraphPad Prizm Software. The K_i, K_m, and IC_{50} values are expressed as mean ± S.E. for three independent measurements.

RESULTS

Mutational Analysis of the Pγ Binding Site of PDE6α′—Previously, we demonstrated that PDE5/PDE6α′ chimeras containing a PDE6α′ sequence, PDE6α′-(737–784), are effectively inhibited by Pγ, and two residues, Met^{758} and Gln^{752}, participate in the inhibitory interaction (6). Based on the model structure of PDE6α′ (6), three solvent-exposed nonconserved PDE6α′ residues, Lys^{769}, Phe^{777}, and Phe^{781}, were chosen for further mutational analysis of the Pγ binding region (Fig. 1*A*). A PDE5/PDE6α′ chimera, Chi16 (6), served as a template for single substitutions of these residues by Ala. The Chi16 mutants were expressed in Sf9 insect cells and partially purified. Expression of the K769A, F777A, and F781A mutants have yielded similar amounts of soluble protein (50–100 μg/100 ml of culture). Neither of these mutations has significantly affected the catalytic properties of chimeric PDE. The K_m and k_{cat} values for cGMP hydrolysis for all three mutants were in the 3–10 μM range, and the 5–10 s^{-1} range, respectively (Table I).

TABLE I
Functional properties of PDE5/PDE6α′ chimeras

PDE activity was measured using [^{3}H]cGMP (24). The K_m values of PDE6α′ or PDE5 and PDE5/PDE6α′ chimeras were determined in the presence of 0.1 μCi [^{3}H]cGMP and 0.1–500 μM of unlabeled cGMP. The K_i and IC_{50} values for inhibition of PDE activity by Pγ and zaprinast were measured using 0.5 μM cGMP. The results are presented as the mean ± S.E. for three independent measurements.

PDE	K_m	k_{cat}	IC_{50} for zaprinast	K_i for Pγ	K_i for PγI86A	K_i for PγI87A
	μM	s^{-1}	μM	nM (*max. effect, %*)	nM (*max. effect, %*)	nM (*max. effect, %*)
PDE6α′	23 ± 2[a]	3500[a]	0.28 ± 0.05[a]	0.17 ± 0.02 (100)[a]	0.75 ± 0.08 (95)	0.65 ± 0.04 (100)
Chi16	2.8 ± 0.5[b]	9.0[b]	0.12 ± 0.01[b]	3.6 ± 0.4 (90)[b]	13 ± 1 (65)	6.6 ± 1.0 (70)
K769A	2.2 ± 0.2	8.9	0.16 ± 0.01	2.9 ± 0.4 (90)		
F777A	4.8 ± 0.7	7.2	0.19 ± 0.01	19 ± 2 (45)	96 ± 13 (45)	64 ± 8 (25)
F781A	6.1 ± 0.7	7.5	0.28 ± 0.02	31 ± 5 (65)	49 ± 8 (40)	32 ± 2 (55)
M758A	9.5 ± 0.9[b]	8.9[b]	0.26 ± 0.01[b]	97 ± 10 (75)[b]	N/A (<20)	N/A (<20)
PDE5	3.3 ± 0.4[a]	9.6[a]	0.54 ± 0.02			
A608G/A612G	14 ± 1	105	0.30 ± 0.03			
Chi20	12 ± 1	116	0.35 ± 0.05			
Chi21	17 ± 2	110	0.39 ± 0.05			

[a] The data are from Ref. 5.
[b] The data are from Ref. 6.

As an additional control for the structural integrity of the catalytic site, mutants of Chi16 were tested for the PDE activity inhibition by zaprinast, a specific competitive inhibitor of PDE5 and PDE6. The largest change, a 2-fold increase in the IC_{50} value, was caused by the F781A substitution (Table I). Nonetheless, such a change represents an insignificant loss of affinity to zaprinast.

The test of the ability of Chi16 mutants to be inhibited by Pγ showed that the K769A mutation had no effect on the inhibitory interaction with Pγ (K_i 2.9 nM) (Table I). Two other mutants, F777A and F781A, displayed significant impairments in the inhibition by Pγ. The F777A substitution reduced both the maximal inhibition of PDE activity by Pγ (~45%) and the K_i value (K_i of 19 nM). The inhibition of F781A mutant by Pγ also was incomplete (~65%) and associated with an increase in the K_i value (K_i of 31 nM) (Fig. 2*A* and Table I).

Effects of the C-terminal Pγ Mutants on the Catalytic Activity of Mutant Chi16—C-terminal Pγ mutants were designed based on the evidence for the critical role of the Pγ C terminus in PDE6 inhibition (21, 28). The two extreme C-terminal Pγ residues, Ile^{86} and Ile^{87}, were replaced by Ala to obtain the PγI86A and PγI87A mutants, respectively. The Pγ mutants were analyzed for their ability to inhibit trypsin-activated PDE6α′ (tPDE), Chi16, and the M758A, F777A, and F781A mutants (Fig. 2; Table I). PγI86A and PγI87A fully inhibited tPDE activity. However, the potency of the inhibition was reduced ~4–5-fold (K_i of 0.75 nM for PγI86A and K_i of 0.65 nM for PγI87A, compared with K_i of 0.15–0.2 nM for Pγ). A similar increase in the K_i values was observed from the inhibition of Chi16 activity by PγI86A (K_i of 13 nM) and PγI87A (K_i of 7 nM) (Fig. 2, *B* and *C*; Table I). Yet, PγI86A and PγI87A did not fully inhibit Chi16, maximal inhibition was 65 and 70%, respectively. (Fig. 2, *B* and *C*; Table I). No appreciable inhibition of M758A by either Pγ mutant was seen even at inhibitor concentrations as high as 5 μM. The inhibition of F777A by PγI86A was partial (45%) with the K_i value of 96 nM, whereas PγI87A inhibited this Chi16 mutant with an even smaller maximal effect (25%, K_i of 64 nM). The F781A mutant was inhibited by PγI86A and PγI87A with K_i values of 49 and 32 nM and maximal effects of 40 and 55%, respectively (Fig. 2, *B* and *C*; Table I).

Catalytic Properties of PDE5/PDE6α′ Chimeras Containing the PDE6α′ Metal Binding Sites—Two conserved metal binding motifs found in all PDEs are absolutely critical for cyclic nucleotide hydrolytic activity (18–20). To identify the structural elements responsible for the unique catalytic properties of PDE6, chimeric PDE5/PDE6α′ have been generated by introduction into PDE5 of PDE6α′ domains containing metal binding motifs, I and II. A replacement of the PDE6α′-(562–617) segment into PDE5 yields a chimeric PDE5/PDE6α′, Chi20, that incorporates both PDE6α′ metal binding sites and the connecting sequence (Fig. 1*A*). Chi20 was expressed in Sf9 cells as a functional enzyme at ~400 μg/100 ml and purified to ~65–70% purity (Fig. 1*B*). The catalytic characteristics of Chi20 were examined in comparison to those of PDE5 and native PDE6α′. PDE6α′ has reported K_m (17–25 μM) and k_{cat} (3500–4500 moles of cGMP per mole of PDE·s) values for cGMP hydrolysis that are ~5 and ~400-fold higher than the respective constants for PDE5 (5, 10–11, 14). The catalytic parameters of Chi20 were significantly different from those of PDE5. Chi20 hydrolyzed cGMP with the K_m value of 12 μM, which is ~4-fold higher than the K_m value for PDE5 but similar to that of PDE6α′ (Table I). The maximal activity of 116 moles of cGMP per mole of PDE·s for Chi20 is ~10-fold higher than that of PDE5. Chi20 was inhibited by zaprinast with the IC_{50} value of 0.35 μM, which is comparable with that of PDE5 (Table I).

To determine the role of individual metal binding motifs and their adjacent regions in cGMP hydrolysis by PDE6, we inserted a PDE6α′ fragment corresponding to the helix-α6 (20), PDE6α′-(562–574), into PDE5 (Chi21) (Fig. 1). The catalytic properties of Chi21 and the inhibition by zaprinast (K_m of 17 μM, k_{cat} of 110 moles of cGMP per mole of PDE·s, and IC_{50} 0.39 μM) were similar to those of Chi20.

Catalytic Properties of the PDE5A608G/A612G Mutant—The alignment of sequences from different PDE families corresponding to the α6 helix shows a glycine residue, PDE6α′Gly^{562}, conserved only in photoreceptor PDEs (Fig. 3*A*). A second Gly residue, PDE6α′Gly^{566}, is conserved in PDE6α′ and PDE6α, but substituted by Ala in PDE6β and PDE5 (Fig. 3*A*). To test the hypothesis that Gly^{562} and Gly^{566} of PDE6α′ are responsible for the differences in catalytic properties of Chi21 and PDE5, a doubly substituted mutant of PDE5, A608G and A612G, was expressed and purified from Sf9 cells. Similar to Chi20 and Chi21, PDE5A608G/A612G hydrolyzed cGMP with a K_m value of 14 μM and a k_{cat} value of 105 moles of cGMP per mole of PDE·s (Table I).

DISCUSSION

An interaction between PDE6 catalytic and inhibitory Pγ-subunits keeps the visual effector enzyme inhibited in the dark. Previous biochemical studies have established that the γ-subunit of photoreceptor PDE inhibits the enzyme activity by blocking its catalytic site (29). The major inhibitory domain has been localized to the Pγ C terminus (21, 28). Recently, we have demonstrated that Pγ inhibits the activity of PDE5/PDE6α′ chimera, Chi 16, containing residues PDE6α′-(737–784) (6).

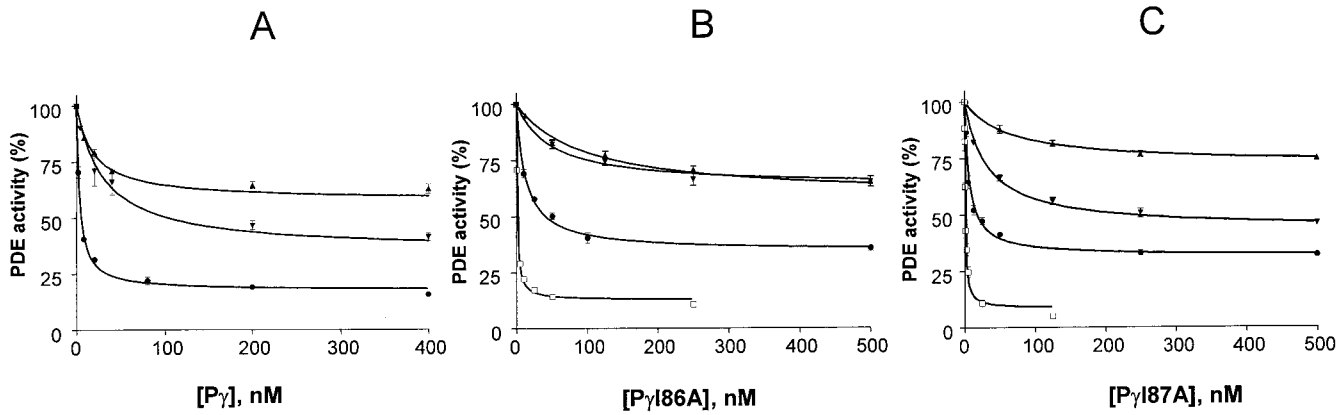

FIG. 2. **Effect of Pγ and C-terminal Pγ mutants on the catalytic activity of tPDE6α′ Chi16 and Chi16 mutants.** *A*, inhibition of Chi16, F777A, and F781A PDE activity by Pγ. The activities of Chi16 (●), F777A (▲), and F781A (▼) (50–100 pM) were determined upon addition of increasing concentrations of Pγ. Reactions were initiated by addition of 0.5 μM of cGMP. The K_i values (nM) calculated from the inhibition curves were 3.6 ± 0.4 (●), 19 ± 2 (▲), and 31 ± 5 (▼). *B*, inhibition of tPDE6α′ (□) (0.5 pM), Chi16 (●), F777A (▲), and F781A (▼) by PγI86A. The K_i values (nM) calculated from the inhibition curves were 0.75 ± 0.08 (□), 13 ± 1 (●), 96 ± 13 (▲), and 49 ± 8 (▼). *C*, inhibition of tPDE6α′ (□), Chi16 (●), F777A (▲), and F781A (▼) by PγI87A. The K_i values (nM) calculated from the inhibition curves were 0.65 ± 0.04 (□), 6.6 ± 1.0 (●), 64 ± 8 (▲), and 32 ± 2 nM (▼).

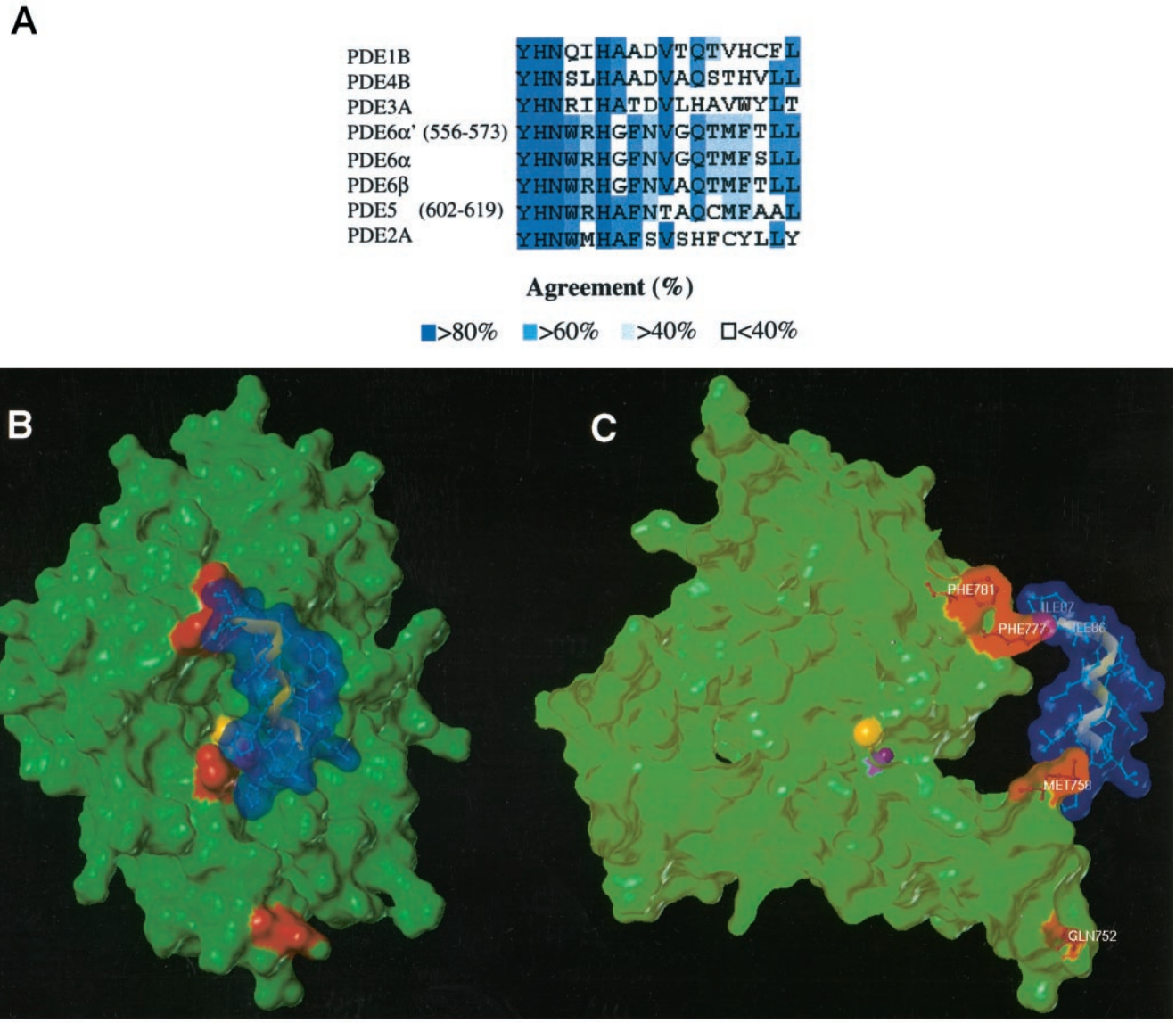

FIG. 3. **The Pγ C terminus docked to the PDE6α′ catalytic site.** *A*, an alignment (31) of PDE1–6 sequences corresponding to the helix-α6 (20). *B* and *C*, a model of the PDE6α′ was generated with SWISS-MODEL (32) using the coordinates of the PDE4 structure as a template (20). The Pγ C terminus binding residues, Gln^{752}, Met^{758}, Phe^{777}, and Phe^{781} are shown in *red*. The metal ions Zn^{2+} and Mg^{2+} are shown in *yellow* and *magenta*, respectively. The C terminus of Pγ, Pγ-(75–87), was generated and manually docked to the catalytic site using SYBYL (v.6.7) (Tripos Associates, St. Louis, MO). *C,* the clipped view is a 90^0 counterclockwise rotation around the vertical axis shown in *B*.

Essential Pγ binding residues, Gln^{752} and Met^{758}, of PDEα' have been identified via mutagenesis of Chi16 (6). A model of the PDE6α' catalytic domain places Met^{758} at the opening of the catalytic pocket (6). Hypothetically, to ensure an effective catalytic block, the Pγ C terminus may lie over or might be inserted into the catalytic cavity. The former appears more likely because the catalytic pockets of different cyclic nucleotide PDEs are made up of highly conserved residues, whereas the inhibition by Pγ is a unique attribute of PDE6. We speculated that to cover the catalytic pocket, the Pγ C terminus, besides Met^{758}, interacts with additional nonconserved residues located at the perimeter of the entrance to the active site. The fact that the introduction of PDE6α'-(737–784) into PDE5/PDE6α' chimera leads to a full inhibition of the PDE activity by Pγ suggests the PDE6α'-(737–784) segment contains most if not all residues interacting with the Pγ C terminus. In the PDE6α' model, PDE6α'-(737–784) comprises about half of the catalytic cavity mouth. Residues at three positions within PDE6α'-(737–784) (Lys^{769}, Phe^{777}, and Phe^{781}) are conserved among photoreceptor PDEs but have nonhomologous substitutions in PDE5. Supporting our hypothesis, replacement of two residues, Phe^{777} and Phe^{781}, by Ala in Chi16 has resulted in mutant PDEs that in comparison with Chi16 were less potently and incompletely inhibited by Pγ. Phe^{777} and Phe^{781} are located next to each other, opposite to the Met^{758} side of the catalytic opening (Fig. 3, *B* and *C*). Thus, it appears that the Pγ C terminus makes a bridge over the catalytic pocket. Such a model provides an interesting explanation to the results of an earlier study that examined inhibition of PDE6 by C-terminally truncated Pγ mutants (21). Truncations of one or two of the C-terminal Ile^{86}-Ile^{87} residues led to substantial increases in the K_i value, whereas further truncations, up to 8–11 C-terminal residues, reduced the maximal inhibition of PDE6 activity without significantly affecting the K_i value (21). A plausible interpretation is that PγIle^{86}-Ile^{87} interact with residues on one side of the catalytic pocket and other residues, perhaps Pγ-(77–85), stretch over the catalytic cavity until Pγ reaches the opposite side. Accordingly, removal of PγIle^{86}-Ile^{87} decreases the affinity of Pγ for the PDE6 catalytic subunit, whereas progressive removal of Pγ-(77–85) residues gradually facilitates access of cGMP to the catalytic site. To determine the orientation of the Pγ C terminus against the catalytic site and identify point-to-point interactions with PDE6α', we examined the inhibition of Chi16 and the M758A, F777A, and F781A mutants of Chi16 by two Pγ mutants, PγI86A and PγI87A. The simplest prediction is that if a C-terminal Ile of Pγ interacts with one of the three PDE6α' residues, the corresponding mutant PDE would be inhibited comparably by Pγ and by the Pγ mutant. Complicating this prediction, side chains of Phe^{777} and Phe^{781} make a hydrophobic contact and thereby may support each other in the interaction with Pγ. The analysis of inhibition of Chi16 mutants by Pγ mutants indicates that Ile^{86} and Ile^{87} of Pγ interact with Phe^{777} and Phe^{781} of PDE6α'. Moderate increases in the K_i values and reductions in the maximal inhibition of F777A and F781A caused by the PγI86A substitution suggest that Ile^{86} probably contacts one or both the PDE6α' residues. The failure of PγI86A to inhibit M758A is consistent with the notion that Ile^{86} binds $Phe^{777/781}$, but not Met^{758}. The lack of inhibition is likely caused by the inability of M758A and PγI86A to establish at least two of the three critical contacts involving Met^{758}, Phe^{777}, and Phe^{781}. The PγI87A mutant did not appreciably inhibit the activity of the M758A mutant PDE. PγI87A inhibited F781A stronger than F777A pointing to a probable contact between PγIle^{87} and Phe^{781} of PDE6α'. The incomplete inhibition of mutant PDEs by Pγ or Pγ mutants most likely reflects equivalent partial inhibition of both active sites of the catalytic dimer, rather than the loss of inhibition at one site.

The analysis of Pγ secondary structure predicts an α-helical structure for the C-terminal residues Pγ-(75–84) (30). The C terminus of Pγ, Pγ-(75–87), manually docked to the PDE6α' catalytic site is shown in Fig. 3, *B* and *C*. The model assumes the helical structure of Pγ-(75–84) and the contacts between PγIle^{86}-Ile^{87} and PDE6$\alpha'$$Phe^{777}$-$Phe^{781}$. This orientation of Pγ is also consistent with Gln^{752} of PDE6α' (6) making a contact with a Pγ residue located N-terminally to Pγ-(75–87).

The remarkable ability of photoreceptor PDEs to hydrolyze cGMP with a catalytic rate constant of ~4000–5500 moles of cGMP per mole of PDE·s (12–15) is essential to the signal amplification in the visual cascade. All catalytic subunits of cyclic nucleotide PDEs contain two strictly conserved metal binding motifs, His-Asn-*X*-*X*-His (motif I) and His-Asp-*X*-*X*-His (motif II). In PDE6α' these motifs are as follows: ^{557}His-Asn-Trp-Arg-His^{561} and ^{597}His-Asp-Ile-Asp-His^{601}. The crucial role of the metal ions and the binding motifs for PDE catalytic activity has been recently supported by a crystallographic study of the PDE4 catalytic domain (20). Rather than forming separate metal binding sites, both motifs are involved in coordination of two bound metal ions, ME1 and ME2 (20). For example, ME1, most likely a tightly bound Zn^{2+}, is coordinated by the His residue (His^{561} of PDE6α') from motif I, and the His and Asp residues from motif II (His^{597}-Asp^{598}). A model of cAMP docked in the PDE4 active site demonstrates that ME1 and ME2 bind the cyclic phosphate, position a potential water molecule for the nucleophilic attack, and would serve to stabilize the transition state (20). In view of the role of metal binding sites in hydrolysis of cyclic nucleotides, we have considered the motifs I and II as probable structural determinants of the catalytic properties of PDE6. Motifs I and II are practically identical in PDE5 and PDE6. Therefore, a spatial orientation of these sites might be a potential key factor for cGMP hydrolysis. Motif I comprises the N-terminal potion of the helix-α6, and motif II is in the loop connecting helices 7 and 8. A PDE5/PDE6α' chimera, Chi20, was generated by replacing a PDE6α' domain containing helices α6-α8 into PDE5. The analysis of Chi20 revealed a more than 10-fold increase in the maximal catalytic rate accompanied by a ~5-fold increase in the K_m value. Subsequent chimeric PDE, Chi21, containing only helix α6 of PDE6α' displayed catalytic properties similar to those of Chi20. An alignment of sequences of photoreceptor PDEs and PDE5 corresponding to the helix-α6 shows a high degree of homology with the notable exception of residues at two positions corresponding to PDE6α' Gly^{562} and Gly^{566}. Gly^{562} of PDE6α' is conserved only in the PDE6 family, but substituted by Ala in PDE5 (Fig. 3*A*). Importantly, Gly^{562} immediately follows His^{561} from motif I. His^{561}, by analogy to PDE4, is involved in coordination of ME1, and in the positioning of His^{557} to accomplish the protonation of the O3′ leaving group (20). To probe the role of the Gly residues, a doubly substituted PDE5 mutant, A608G/A612G, has been made. The k_{cat} value of the A608G/A612G mutant was comparable with those of Chi20 and Chi21, and ~10-fold higher then that of PDE5. These results suggest that the Gly residues are in part responsible for the catalytic characteristics of PDE6. Most likely, they allow for a positioning of motif I that is most favorable for cGMP hydrolysis. Other yet to be defined determinants contribute to the unique catalytic power of PDE6, because the achieved k_{cat} value is still ~40–50-fold lower than k_{cat} described for native activated PDE6. Overall, our results suggest that a progressive incorporation of PDE6 domains or residues into PDE5 not only allows a structure-function analysis of PDE6, but also repre-

sents a realistic approach to generate a chimeric enzyme that would be functionally indistinguishable from PDE6.

Acknowledgment—We thank Boyd Knosp for assistance with molecular modeling.

REFERENCES

1. Chabre, M., and Deterre, P. (1989) *Eur. J. Biochem.* **179,** 255–266
2. Yarfitz, S., and Hurley, J. B. (1994) *J. Biol. Chem.* **269,** 14329–14332
3. Piriev, N. I., Yamashita, C., Samuel, G., and Farber, D. (1993) *Proc. Natl. Acad. Sci. U. S. A.* **90,** 9340–9344
4. Qin, N., and Baehr, W. (1994) *J. Biol. Chem.* **269,** 3265–3271
5. Granovsky, A. E., Natochin, M., McEntaffer, R. L., Haik, T. L., Francis, S. H., Corbin, J. D, and Artemyev, N. O. (1998) *J. Biol. Chem.* **273,** 24485–24490
6. Granovsky, A. E., and Artemyev, N. O. (2000) *J. Biol. Chem.* **275,** 41258–41262
7. McAllister-Lucas, L. M., Sonnenburg, W. K., Kadlecek, A., Seger, D., Trong, H. L., Colbran, J. L., Thomas M. K., Walsh, K. A., Francis, S. H., Corbin, J. D., and Beavo, J. A. (1993) *J. Biol. Chem.* **268,** 22863–22873
8. Gillespie, P. G., and Beavo, J. A. (1989) *Mol. Pharmacol.* **36,** 773–781
9. Turko, I. V., Ballard, S. A., Francis, S. H., and Corbin, J. D. (1999) *Mol. Pharmacol.* **56,** 124–130
10. Thomas, M. K., Francis, S. H., and Corbin, J. D. (1990) *J. Biol. Chem.* **265,** 14964–14970
11. Turko, I. V., Francis, S. H., and Corbin, J. D. (1998) *J. Biol. Chem.* **273,** 6460–6466
12. Mou, H., Grazio, H. J., III, Cook, T. A., Beavo, J. A., and Cote, R. H. (1999) *J. Biol. Chem.* **274,** 18813–18820
13. Leskov, I. B., Klenchin, V. A., Handy, J. W., Whitlock, G. G., Govardovskii, V. I., Bownds, M. D., Lamb, T. D., Pugh, E. N., and Arshavsky, V. Y. (2000) *Neuron* **27,** 525–537
14. Gillespie, P. G., and Beavo, J. A. (1988) *J. Biol. Chem.* **263,** 8133–8141
15. Dumke, C. L., Arshavsky, V. Y., Calvert, P. D., Bownds, M. D., and Pugh, E. N., Jr. (1994) *J. Gen. Physiol.* **103,** 1071–1098
16. Turko, I. V., Haik, T. L., McAllister-Lucas, L. M., Burns, F., Francis, S. H., and Corbin, J. D. (1996) *J. Biol. Chem.* **271,** 22240–22244
17. Artemyev, N. O., Natochin, M., Busman, M., Schey, K. L., and Hamm, H. E. (1996) *Proc. Natl. Acad. Sci. U. S. A.* **93,** 5407–5412
18. Francis, S. H., Turko, I. V., Grimes, K. A., and Corbin, J. D. (2000) *Biochemistry* **39,** 9591–9596
19. He, F., Seryshev, A. B., Cowan, C. W., and Wensel, T. G. (2000) *J. Biol. Chem.* **275,** 20572–20577
20. Xu, R. X., Hassell, A. M., Vanderwall, D., Lambert, M. H., Holmes, W. D., Luther, M. A., Rocque, W. J., Milburn, M. V., Zhao, Y., Ke, H., and Nolte, R. T. (2000) *Science* **288,** 1822–1825
21. Skiba, N. P., Artemyev, N. O., and Hamm, H. E. (1995) *J. Biol. Chem.* **270,** 13210–13215
22. Artemyev, N. O., Arshavsky, V. Y., and Cote, R. H. (1998) *Methods* **14,** 93–104
23. Thompson, W. J., and Appleman, M. M. (1971) *Biochemistry* **10,** 311–316
24. Natochin, M., and Artemyev, N. O. (2000) *Methods Enzymol.* **315,** 539–554
25. Bradford, M. M. (1976) *Anal. Biochem.* **72,** 248–254
26. Laemmli, U. K. (1970) *Nature* **227,** 680–685
27. Towbin, H., Staehelin, T., and Gordon, J. (1979) *Proc. Natl. Acad. Sci. U. S. A.* **76,** 4350–4354
28. Brown, R. L. (1992) *Biochemistry* **31,** 5918–5925
29. Granovsky, A. E., Natochin, M., and Artemyev, N. O. (1997) *J. Biol. Chem.* **272,** 11686–11689
30. Rost, B. (1996) *Methods Enzymol.* **266,** 525–539
31. Thompson J. D., Higgins D. G., and Gibson T. J. (1994) *Nucleic Acids Res.* **22,** 4673–4680
32. Guex, N., and Peitsch, M. C. (1997) *Electrophoresis* **18,** 2714–2723

Partial Reconstitution of Photoreceptor cGMP Phosphodiesterase Characteristics in cGMP Phosphodiesterase-5

Alexey E. Granovsky and Nikolai O. Artemyev

J. Biol. Chem. 2001, 276:21698-21703.
doi: 10.1074/jbc.M100626200 originally published online April 2, 2001
